European Journal of Agronomy 103 (2019) 73–79

Contents lists available at ScienceDirect

European Journal of Agronomy

journal homepage: www.elsevier.com/locate/eja

Rice exposure to cold stress in China: how has its spatial pattern changed under climate change?

Pin Wang[a,b], Tangao Hu[a,b], Feng Kong[c], Junfeng Xu[a,b], Dengrong Zhang[a,b,*]

[a] Institute of Remote Sensing and Earth Sciences, College of Science, Hangzhou Normal University, Hangzhou 311121, China
[b] Zhejiang Provincial Key Laboratory of Urban Wetlands and Regional Change, Hangzhou 311121, China
[c] School of Public Policy and Management, Tsinghua University, Beijing 100084, China

ARTICLE INFO

Keywords:
Cold stress
Rice
Geographical centroid
Climate change
China

ABSTRACT

Extreme cold events have always been great threats to the major rice-cultivation areas across China. The spatial pattern of rice exposure to cold stress (ECS) is critical to develop countrywide adaptation strategies. Under climate change, whether and how ECS spatial pattern has changed? These answers are urgently required for adaptation optimization, but regrettably remain unclear. Here, we examined the changes in rice-planted area exposed to cold stress across mainland China, and historical movements of the geographical centroids of rice ECS over 1980–2015. The results showed that in the single rice cultivation of northeast China and the Yunan-Guizhou plateau, the area exposed to cold stress has shrunk significantly and the centroid moved northward since the 1980s. The southern parts of the mid-lower reaches of Yangtze River witnessed a continuous decrease in the area exposed to cold stress from the 1980s to 2000s, but a large expansion over the 2010s. In south China, the areas exposed to cold stress mainly gathered in the northern parts and showed large variations since the 1980s. These two regions dominant by double rice have witnessed westward movements of ECS centroids over the past decades.

1. Introduction

Rice (*Oryza sativa* L.), one of the most important food crops worldwide (Iizumi et al., 2017; Zhao et al., 2017), is highly sensitive to extreme low temperatures (Lesk et al., 2016; Espe et al., 2017). Panicle tip degeneration, incomplete panicle exertion, high spikelet sterility and irregular maturity would be caused by cold events particularly during rice booting and heading-flowering stages (Sánchez et al., 2014; Arshad et al., 2017; Espe et al., 2017). As the world's largest rice producer, China has been hit by frequent cold events particularly in northeastern region (Sun et al., 2017; Zhang et al., 2017a), where an average loss of rice production in 1969, 1972 and 1976 reached up to 5.78 million tons (about 20% of total production) (Wang, 2008). Urgently, countrywide adaptation strategies should be developed on the basis of the spatial pattern of rice exposure to cold stress (ECS) across China (Zhang et al., 2014, 2017a). Under global warming (Stott, 2016), significant changes in ECS intensity over the past decades have been found (Zhang et al., 2014; Wang et al., 2016), which inevitably led to changes in ECS spatial pattern and consequently important adjustments in adaptation measures. Therefore, a sound understanding of the changes in ECS spatial pattern across mainland China over the past decades, could help to optimize adaptive measures for addressing cold-stress threats, furthermore provides critical insights into how the system is likely to respond in the future.

Under climate change, how did ECS spread across the major rice-cultivation areas in China? Where did the hardest-hit areas move over the past decades? These problems are critical to help understand the changes in ECS spatial pattern. Recently, several studies have been conducted to reveal the spatio-temporal pattern of rice ECS across China. For example, in Sun and Huang's study (2011), the study area was divided into five regions, and the decadal changes of ECS intensity were analyzed for each region. But regrettably, the detailed spatial pattern has not been revealed. To fill this gap, Zhang et al. (2014) adopted similar zoning method across China, and depicted the spatial pattern of average annual ECS intensity and its temporal trends over 1960–2009. Their findings mainly described the spatial pattern of rice ECS over the entire time period, but could hardly reveal its changes between different decades. In Tao et al.'s study (2013), some clues about the changes in ECS spatial pattern could be captured at the station scale, from the occurrence-frequency differences of extreme cold events between the 1990s and 2000s. But more detailed analysis about the changes in ECS spatial pattern could not be found, subject to the

* Corresponding author at: Institute of Remote Sensing and Earth Sciences, College of Science, Hangzhou Normal University, Hangzhou 311121, China.
E-mail address: zhangdengrong2017@126.com (D. Zhang).

https://doi.org/10.1016/j.eja.2018.11.004
Received 21 June 2018; Received in revised form 10 November 2018; Accepted 13 November 2018
Available online 06 December 2018
1161-0301/ © 2018 Elsevier B.V. All rights reserved.

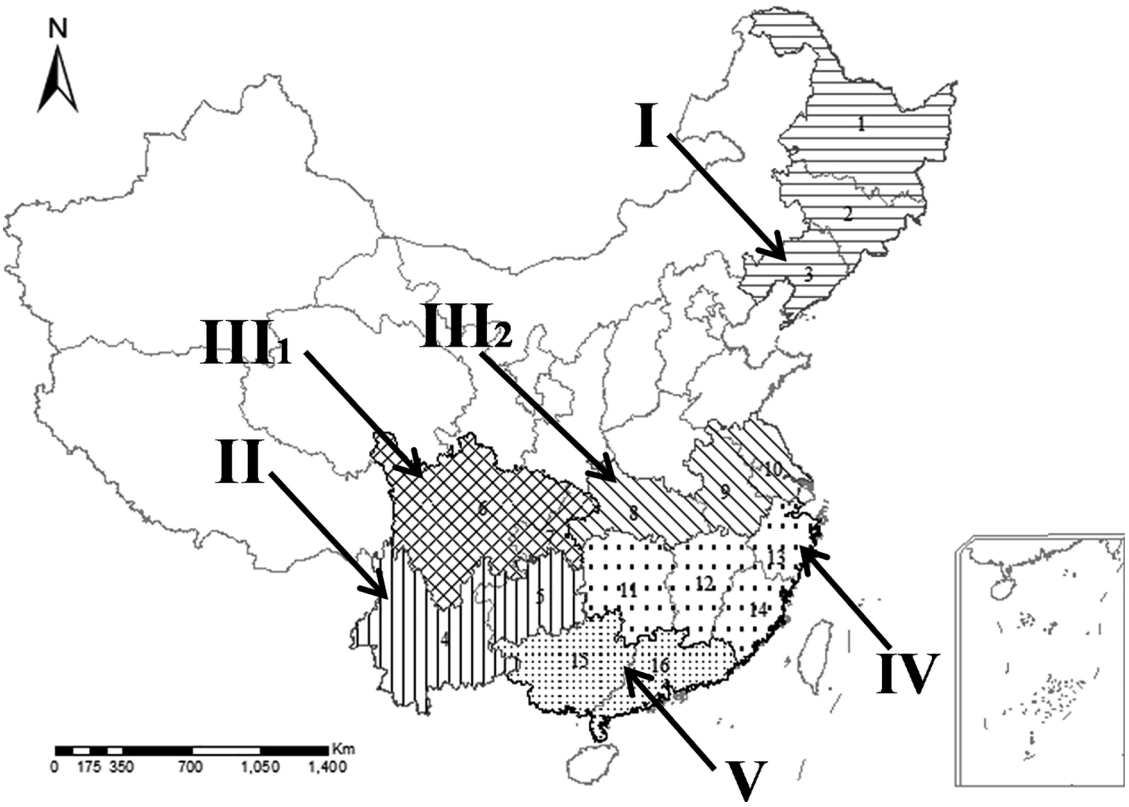

Fig. 1. Spatial distribution of rice cultivation in the study area. I single rice in northeast China; II single rice in the Yunnan-Guizhou Plateau; III single rice in the Sichuan Basin (III_1, including Sichuan and Chongqing provinces) and the north of mid-lower reaches of the Yangtze River (III_2, including Hubei, Anhui and Jiangsu provinces); IV double rice in the south of mid-lower reaches of the Yangtze River; V double rice in south China. Province codes: 1 Heilongjiang; 2 Jilin; 3 Liaoning; 4 Yunnan; 5 Guizhou; 6 Sichuan; 7 Chongqing; 8 Hubei; 9 Anhui; 10 Jiangsu; 11 Hunan; 12 Jiangxi; 13 Zhejiang; 14 Fujian; 15 Guangxi; 16 Guangdong. The map inset describes the South China Sea.

station scale and the study period (1990–2009) used in their study. In summary, the problems above have not been well solved, leading to the changes in rice-ECS spatial pattern over the past decades across mainland China still unclear.

Therefore, efforts would be made here to assess the decadal changes in ECS spatial pattern over 1980–2015 across the major rice-cultivation areas in mainland China. Based on the datasets of meteorology and rice crop, we aimed to: (i) analyze the decadal changes in rice-planted area exposed to cold stress; (ii) reveal the historical movements of the geographical centroids of rice ECS; (iii) gain insight into the underlying mechanisms of the centroid movements and discuss potential adaptation measures.

2. Materials and methods

2.1. Study area and data sources

According to several related studies (Sun and Huang, 2011; Zhang et al., 2014, 2017a), sixteen provinces frequently hit by cold events were included in this study (Fig. 1). These areas could be divided into five regions, including Region I (northeast China), Region II (the Yunnan-Guizhou Plateau), Region III (including the Sichuan Basin (III_1) and the northern parts of the mid-lower reaches of Yangtze River (III_2)), Region IV (the southern parts of the mid-lower reaches of Yangtze River) and Region V (south China). Over the past decades, single rice was dominant in Region I, II and III, while double rice in Region IV and V. The counties with more than ten years of rice-yield records were selected into the study area. Daily temperature data over 1980–2015 were obtained from the weather stations of the China Meteorological Administration, including daily minimum temperature (T_{min}) and daily maximum temperature (T_{max}). In the study area, weather stations are densely distributed, so daily temperatures in each county were computed from its nearest weather station.

2.2. Calculation of rice ECS

When calculating rice ECS, the booting and heading-flowering stages were included in the thermal-sensitive period (TSP, days), since cold stress during these two stages was recognized to significantly associated with reduced crop yields (Sun and Huang, 2011; Liu et al., 2013; Espe et al., 2017). In Region IV and V, the TSP of early rice was mainly in summer (including July and August) when rice plants are frequently hit by heat events rather than cold events, so early-rice exposure to cold stress has not be considered; only late-rice exposure to cold stress was taken into consideration, since the TSP of late rice tends to overlap with cold dew winds in autumn (Sun and Huang, 2011; Qian et al., 2015). Based on previous studies (Sun and Huang, 2011; Liu et al., 2013; Zhang et al., 2014), the threshold of ECS in each region was listed in Table 1. And the phenological records in different regions were determined following Sun and Huang's study (2011) (see Table S1 in the Supplementary Materials)

In this study, the quantitative index of CDD was introduced to characterize the occurrence and intensity of rice ECS. According to Zhang et al.'s study (2014), the calculation of CDD in a given year could be divided into three steps: firstly, identify the occurrence frequency of extreme low temperature events over a given growth stage; then, compute daily cold-stress exposure (DD) for each event; finally, these daily values of DD were accumulated to calculate the intensity of cold-stress exposure (CDD) in this growth stage. Since the TSP included two critical stages, ECS during each stage should be firstly computed in isolation and then added up for rice ECS during the whole TSP.

Table 1
Thresholds of extreme low temperature events in different rice-planted regions[a].

Growth stage	Region codes		
	I	II and III	IV and V
Booting	At least 2 successive days with a mean daily T ≤ 17°C	At least 3 successive days with a mean daily T ≤ 20°C	At least 3 successive days with a mean daily T ≤ 20°C
Heading-flowering	At least 2 successive days with a mean daily T ≤ 19°C	At least 3 successive days with a mean daily T ≤ 20°C	At least 3 successive days with a mean daily T ≤ 22°C

[a] Data sources: Sun and Huang (2011); Zhang et al. (2014). The region codes were marked in Fig. 1.

$$DD_{i,j} = \begin{cases} T_{base} - T_{i,j} & for \ \ T_{i,j} \le T_{base} \\ 0 & for \ \ T_{i,j} > T_{base} \end{cases} \quad (1)$$

$$CDD = \sum_{j=1}^{n} \sum_{i=1}^{k} DD_{i,j} \quad (2)$$

Where $DD_{i,j}$ (°C) indicates daily cold-stress exposure on the i^{th} day of the j^{th} event; $T_{i,j}$ is the average of daily minimum temperature and daily maximum temperature; T_{base} is the low-temperature threshold of extreme events (Table 1); n is the occurrence frequency of extreme low temperature events over a given growth stage; k is the duration of the j^{th} extreme event.

2.3. Analysis of decadal changes in ECS spatial pattern

Both the areas exposed to cold stress (hereinafter, ECS area) and the geographical centroids of ECS intensity (hereinafter, ECS centroid) were analyzed to explore the decadal changes in ECS spatial pattern. The study period of 1980–2015 was divided into four decades, including the 1980s (1980–1989), 1990s (1990–1999), 2000s (2000–2009) and 2010s (2010–2015).

2.3.1. Areas exposed to cold stress

To ensure ECS area credible, we set standards for its identification: if one county saw extreme cold events in more than one third of a given decade (i.e., $DP \ge 1/3$), it could be identified as a part of ECS area (i.e., $ACS = 1$ in Eq. (3)). In this case, the counties occasionally hit by cold events in a given decade would not be considered. At provincial/regional scale, the percentage of ECS area during a given decade ($ACSP$) could be obtained by Eq. (4). And the $ACSP$ values over different decades were compared to analyze the decadal changes in ECS area.

$$\begin{cases} ACS_j = 1, \ DP_j \ge 1/3 \\ ACS_j = 0, \ DP_j < 1/3 \end{cases} \quad (3)$$

$$ACSP = \frac{\sum_{j=1}^{n} ACS_j}{n} \quad (4)$$

Where j and n indicate the j^{th} county and the total number of counties in a certain province/region, respectively.

2.3.2. Geographical centroids of rice ECS

The centroid method was used to calculate the geographical centroid of rice ECS. We estimated the locations (longitude X and latitude Y) of ECS centroids over a given decade in each region by using Eq. (5) (Li et al., 2015). These geographical centroids were calculated and plotted to indicate historical movements over the past decades, which visually represented the overall changes in the spatial pattern of ECS intensity.

$$\begin{cases} X_T = \frac{\sum_{i=1}^{n}(CDD_{i,T} \times x_i)}{\sum_{i=1}^{n} CDD_{i,T}} \\ Y_T = \frac{\sum_{i=1}^{n}(CDD_{i,T} \times y_i)}{\sum_{i=1}^{n} CDD_{i,T}} \end{cases} \quad (5)$$

Where x_i and y_i are the longitude and latitude of the geographical centroid in the i^{th} county, respectively; $CDD_{i,T}$ is the average value of CDD over the T decade in the i^{th} county; n is the total number of the counties in a certain region. When calculating $CDD_{i,T}$, we got rid of the maximum and minimum values during a given decade to reduce the potential impacts of extreme values.

According to Eq. (5), the movement of ECS centroids is mainly due to the changes in the relative levels of ECS intensity in different parts of a certain region. In order to gain insight into the underlying mechanisms, we compared the relative levels of ECS intensity between different decades in a given region by using Eq. (6).

$$Diff_i = \frac{CDD_{i,T}}{\sum_{i=1}^{n} CDD_{i,T}} * 100 - \frac{CDD_{i,T-1}}{\sum_{i=1}^{n} CDD_{i,T-1}} * 100 \quad (6)$$

Where $Diff_i$ (%) indicates the difference in the relative levels of ECS intensity between the T decade and its last decade (T-1) in the i^{th} county; the other characters have the same meanings as those in Eq. (5).

3. Results

3.1. Changes in rice-planted area exposed to cold stress

The percentages of ECS area in each region/province over different decades were listed in Table 2, and the spatial distribution of the change in ECS area between each two decades was illustrated in Fig. 2. From the 1980s to 1990s, the percentage in Region I decreased by 16.9% (from 54.5% to 37.6%), with the area newly freefrom cold stress mainly detected in the south of P1 and the middle of P2; Region II and III did not see large changes in ECS area; the percentage in Region IV dropped by 20.6% (from 73.6% to 53.0%), and the area newly freefrom cold stress was concentrated in P12; in contrast, Region V experienced

Table 2
The percentages (%) of rice-planted area exposed to cold stress in each region/province over the past four decades.

Decades	Region codes						Province codes															
	I	II	III_1	III_2	IV	V	1	2	3	4	5	6	7	8	9	10	11	12	13	14	15	16
1980s	54.5	32.7	7.5	1.7	73.6	23.8	89.9	58.0	5.0	42.9	17.1	9.3	0.0	5.0	0.0	0.0	93.3	84.4	91.0	15.8	40.9	8.3
1990s	37.6	30.8	7.5	1.3	53.0	35.7	74.7	22.0	1.7	41.3	14.6	9.3	0.0	3.8	0.0	0.0	77.1	36.7	73.1	18.4	60.2	13.4
2000s	45.5	26.4	7.5	2.9	37.0	9.2	77.2	48.0	1.7	34.1	14.6	9.3	0.0	8.8	0.0	0.0	69.5	28.9	26.9	11.8	18.2	1.0
2010s	27.5	28.9	7.5	3.4	75.4	21.6	55.7	14.0	1.7	38.1	14.6	9.3	0.0	10.0	0.0	0.0	99.1	84.4	87.2	19.7	35.2	9.3

Note: the region codes and province codes were marked in Fig. 1.

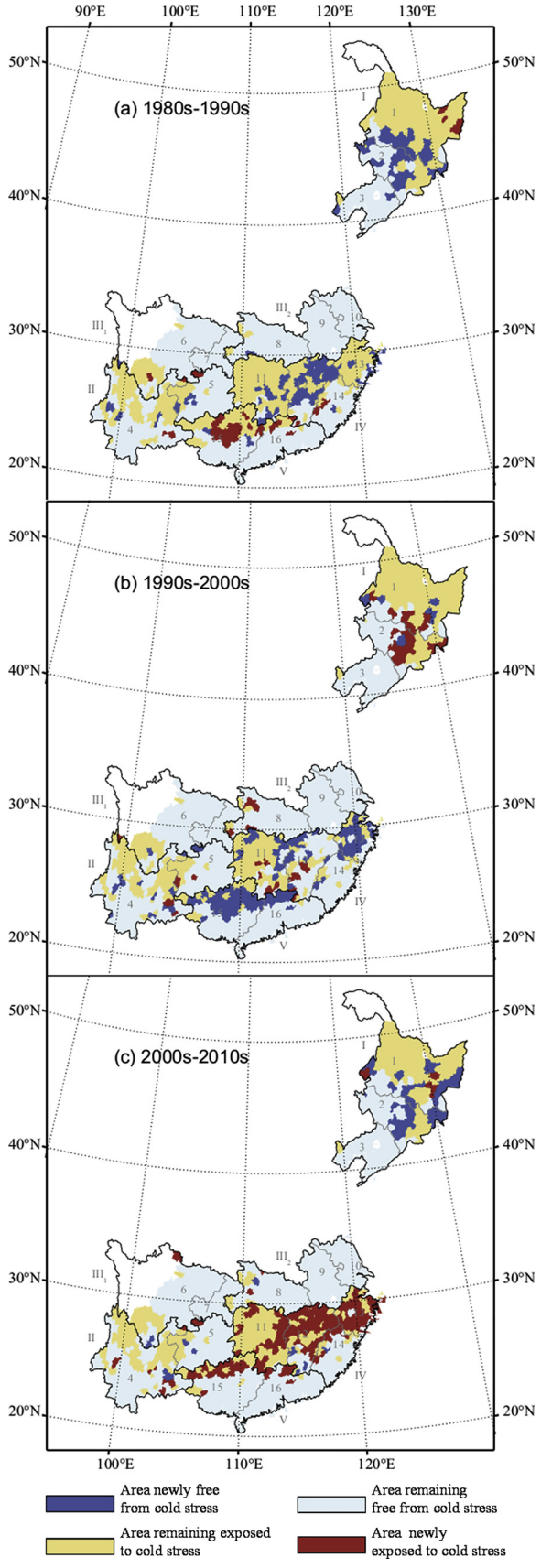

Fig. 2. Changes in rice-planted area exposed to cold stress between different decades. (a) from the 1980s to 1990s; (b) from the 1990s to 2000s; (c) from the 2000s to 2010s.

an increase of 11.9% in ECS area (from 23.8% to 35.7%) and the newly-exposed area was distributed in the north of P15 and P16. From the 1990s to 2000s, the percentage increased by 7.9% (from 37.6% to 45.5%) in Region I, mainly due to the newly-exposed area in the middle of P2; similarly, the west of Region III_2 was also newly exposed to cold stress, resulting in a slight growth (1.6%) in ECS area; in contrast, Region IV and V witnessed significant decreases of 16.0% (from 53.0% to 37.0%) and 26.5% (from 35.7% to 9.2%), respectively, and the area newly free from cold stress was mainly found in the most of P13 and the north of P15. From the 2000s to 2010s, only the percentage in Region I decreased significantly by 18.0% (from 45.5% to 27.5%); the other regions witnessed increases in ECS area, particularly Region IV (from 37.0% to 75.4%) and Region V (from 9.2% to 21.6%). In Region I, the area newly free from cold stress was mainly found in the south of P1 and the middle of P2; in Region IV and V, the area newly exposed to cold stress was detected in the most of P12 and P13, and the northern parts of P15.

3.2. Movements of the geographical centroids of rice ECS

The movement of ECS centroids in each region over the past decades was shown in Fig. 3, and the corresponding directions and linear distances were listed in Table 3. In Region I, the centroid moved 96.6 km northeastward (longitude 0.9°E, latitude 0.7°N) from the 1980s to 1990s, then 111.6 km southwestward (longitude 0.3°W, latitude 1.0°S) from the 1990s to 2000s and 68.9 km northwestward (longitude 0.3°W, latitude 0.6°N) from the 2000s to 2010s. Overall, the centroids were located in P1 and moved northward over the past decades. Region II saw the ECS centroids mainly in northern P4, where a northward movement was found since the 1980s. In Region III_1, the centroids wandered in the south of P6, and the movements were relatively small indicated by the distance no larger than 26.0 km. Similarly, the ECS centroids in Region III_2 were also concentrated in a small portion of western P8, and their movements were small and irregular. In Region IV, the centroid moved 62.5 km southwestward (longitude 0.6°W, latitude 0.2°S) from the 1980s to 1990s, and then continued to move 115.4 km southwestward (longitude 0.1°W, latitude 0.5°S) from the 1990s to 2000s and 48.5 km northeastward (longitude 0.1°E, latitude 0.4°N) from the 2000s to 2010s. Overall, the centroids in Region IV

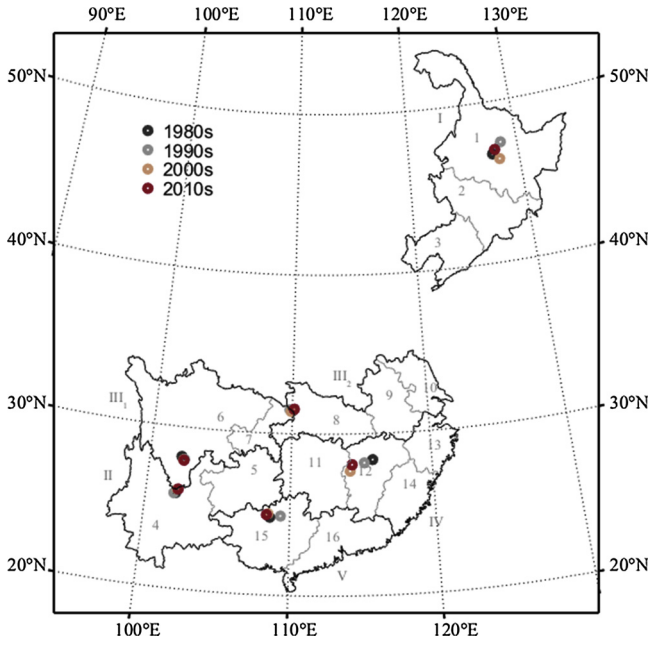

Fig. 3. Geographical centroids of rice-ECS intensity in different regions over the past four decades.

Table 3
Movements of ECS centroids between different decades in each region[a].

	Region I			Region II			Region III_1			Region III_2			Region IV			Region V		
	lon	lat	dis	lon	lat	dis	lon	lat	dis	lon	lat	dis	lon	lat	dis	lon	lat	dis
1980s-1990s	0.9	0.7	96.6	−0.1	0.0	13.3	0.2	−0.1	26.0	−0.2	0.0	23.4	−0.6	−0.2	62.5	0.7	0.1	76.5
1990s-2000s	−0.3	−1.0	111.6	0.2	0.3	36.9	−0.1	0.0	8.3	0.1	−0.1	15.2	−1.0	−0.5	115.4	−0.9	0.1	89.8
2000s-2010s	−0.3	0.6	68.9	0.1	0.0	6.0	0.0	0.0	4.2	0.2	0.2	27.4	0.1	0.4	48.5	−0.1	−0.1	13.1

[a] "lon", "lat" and "dis" represent the movement in longitude (°N), latitude (°E) and linear distance (km), respectively.

were located in the north of P12 and showed a significant westward movement since the 1980s. In Region V, the centroid moved 76.5 km northeastward (longitude 0.7°E, latitude 0.1°N) from the 1980s to 1990s, and then moved westward continuously from the 1990s to 2010s. Overall, the centroids in Region V were concentrated in the north of P15.

3.3. Changes in the intensity of rice ECS

The spatial distribution of changes in the relative levels of rice-ECS intensity (%, calculated by Eq. (6)) over the past decades was illustrated in Fig. 4, to help understand the mechanism underlying the movements of ECS centroids (Fig. 3). From the 1980s to 1990s, ECS intensity in the northern parts of Region I increased by an average of 0.8%, while the other ECS area (including the south of P1 and most of P2) saw decreases ranging from −0.7% to −0.1%. In Region II, an increase of 0.3% on average was found in the northwest of P4. In Region IV, ECS intensity in the eastern parts (including P12 and P13) decreased by an average of −0.2%. In Region V, the north of P15 and P16 saw increases of ECS intensity ranging from 0.1% to 2%. From the 1990s to 2000s, a decrease of −0.8% on average in ECS intensity was found in the northern portions of Region I. In the north of Region II and the south of Region III_1, ECS intensity increased by 0.5% and 0.8% on average, respectively. In Region IV, most of P13 saw a decrease of -0.3% on average, while most of P11 witnessed an increase. ECS intensity in most of northern Region V decreased by the rate ranging from −2% to −0.2%. From the 2000s to 2010s, in Region I, the northwest of P1 saw larger increases in ECS intensity (1.3% on average), while the other ECS area witnessed decreases. In Region II, ECS intensity in the northern parts increased by a range of 0.1%–1.4%. Most of ECS area in Region IV saw increases ranging from 0.1% to 0.6%, whereas only small portions in the south of P11 and P12 witnessed decreases in ECS intensity. In Region V, increases ranging from 0.2% to 3% were found in the north of P15.

4. Discussion

4.1. Changes in the spatial pattern of rice ECS and adaptation strategies

In the single rice growing regions, the ECS area in both Region I and II declined since the 1980s (Fig. 2), and their ECS centroids moved northward over the past decades (Fig. 3). Region III, by contrast, did not see much change/movement in ECS area and ECS centroids (Figs. 2 and 3). Specifically, large parts of Region I (including the south of P1 and the middle of P2) became free from frequent attacks by cold events, whereas only scattered portions of Region II experienced a decrease in the occurrence of extreme cold events (Fig. 2). Consequently, Region I witnessed a much larger decline in ECS area (ranging from 54.5% to 27.5%) than that in Region II (ranging from 32.7% to 28.9%) (Table 2). The northern parts of both Region I and II saw increases in the relative levels of ECS intensity (Fig. 4), so the centroids moved northward over the past decades. Given that ECS area in Region II was much smaller, the movement of ECS centroids in Region I showed a larger extent. In the late rice growing regions, both Region IV and V witnessed a large increase of ECS area over the 2010s, despite continuous decreases in Region IV and larger variations in Region V from the 1980s to 2000s (Fig. 2). The ECS centroids in both two regions moved westward over the past decades (Fig. 3). Specifically, the west of Region IV witnessed increases in the relative level of ECS intensity particularly from the 1980s to 2000s, while the northwest of Region V experienced large increases since the 1990s (Fig. 4).

Overall, these changes in ECS spatial pattern across mainland China indicated that, climate change did reduce cold stress in most of the single rice growing area (particularly at high latitudes), but increased the variations of cold stress in the late rice growing regions (particularly in the area close to coastal lands). Such cases could also be supported by some previous studies. In Sun and Huang's study (2011), the change in ECS intensity from the 1980s to 2000s in Region I was larger than that in Region II. Zhang et al. (2014) found the temporal trend of ECS intensity in the east of Region IV was more significant than that in the western parts during 1960–2009. For single rice, the stages most sensitive to cold stress are often overlap with the warmest periods in summer (July and August), during which the mean temperature has substantially increased and the number of cold days has decreased (Field et al., 2012; Tao et al., 2013; Ren et al., 2017). And in Meng et al.'s study (2014), it was found that latitudes above 45°N have been characterized by rates of warming faster than the global average since 1980. In contrast, in the late rice growing areas, the thermal-sensitive stages are mainly in autumn, during which cold air dips south bringing strong and cold winds (called cold dew winds) (Qian et al., 2015). Despite the warming trend in northern China (Ren et al., 2017), the area close to coastal lands often experienced oceanic winds and air masses which could moderate cold air and hence resulted in large variations of cold wet days (Qian et al., 2015).

In the area which becomes newly free from cold stress over the 2010s (e.g., southern P1), adaptation measures are necessitated to make full use of the favorable conditions. For instance, rapid expansion of rice-planting area and shifts to longer growth-period varieties have been implemented in some portions of Region I (Yang et al., 2007; Li et al., 2015). As for some areas which are newly exposed to cold stress (e.g., P12 and P13), in order to minimize ECS, local farmers could either shift their sowing time or select rice cultivars passing through sensitive growth stages before the onset of cold stress conditions (Chen et al., 2012). Improving cold tolerance of rice cultivars offers substantial hope for coping with an increasing risk of cold stress (Olesen et al., 2011; Moura et al., 2017). Besides, more attentions should be paid to the regions with significant movements of ECS centroids. For example, ECS centroids in Region IV moved westward over the past decades, due to an increase of the relative level of ECS intensity in the western portions. Therefore, greater efforts should be devoted to these parts (mainly in P11), such as developing cold-stress early warning system and crop insurance schemes (e.g., temperature-related weather index for agricultural insurance) (Zhang et al., 2015, 2017b; Sun et al., 2018).

4.2. Limitations in this study

Given the goal of this study is to describe large-scale changes, we assumed a stable threshold for cold stress over the period 1980–2015. But presumably there should be advances in cultivar cold-tolerance during this period. To discuss how changes in cold-tolerance could

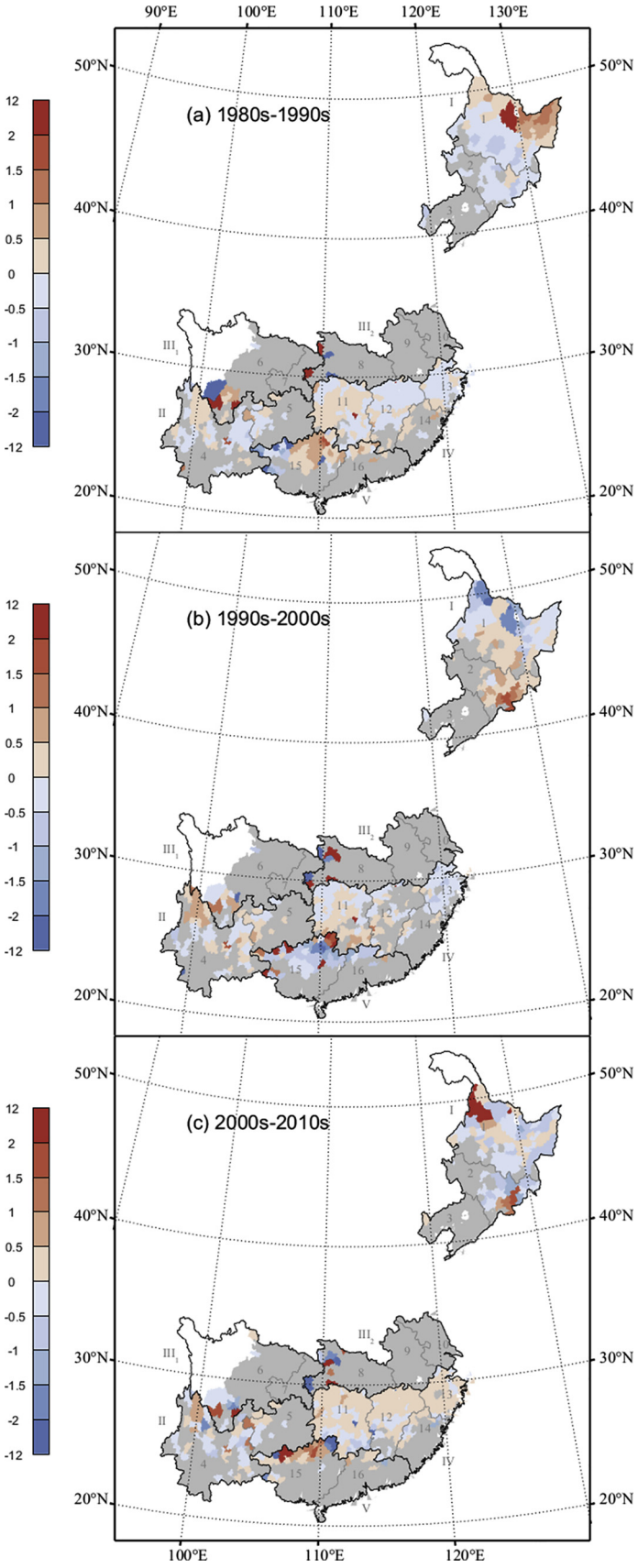

Fig. 4. Changes in the relative levels of rice-ECS intensity (%) between different decades. (a) from the 1980s to 1990s; (b) from the 1990s to 2000s; (c) from the 2000s to 2010s. The area in grey indicates the area free from cold stress in both two decades.

influence the conclusions, a sensitivity test was performed using the method similar to that in Gourdji et al., (2013). We recalculated rice ECS using 1°C/2°C lower critical temperatures than those listed in Table 1, and revealed the changes of their spatial patterns by the methods in Section 2.3. For brevity, the results were illustrated in Fig. S1-S4 (see the Supplementary Materials). As the threshold decreased (i.e., rice cold-tolerance increased), the ECS area did decrease significantly and the locations of ECS centroids showed a little change in each decade. But the decadal changes in ECS area and the movements of ECS centroids were consistent with current conclusions.

Besides, during the process of interpolating temperature data from stations to counties, some factors not considered here (e.g., micro-climate), might influence the calculations of CDD and then lead to some uncertainties in the changes of ECS spatial pattern at the county scale. So the resulting broad-scale analysis is more suited to capturing major patterns at a larger scale (e.g., provinces or regions), than be interpreted at a fine county scale. To further address the uncertainties in small-scale analysis, better weather observation systems in China should be built for climate-change studies.

5. Conclusions

Based on the quantitative index of CDD, the decadal changes in the spatial pattern of rice ECS across mainland China over 1980–2015 were studied. In the single rice growing area, both Region I and II saw continuous declines since the 1980s, and their ECS centroids moved northward over the past decades. In Region III, by contrast, the ECS area was found in a small portion, resulting in little changes/movements of ECS area centroids. In the late rice growing area, both Region IV and V witnessed a large expansion of ECS area over the 2010s, despite continuous decreases in Region IV and large variations in Region V from the 1980s to 2000s. And the ECS centroids in both two regions moved westward since the 1980s.

In the grander scale, understanding how the spatial pattern of rice ECS - both in terms of ECS area and centroids - has historically responded to climate change, will provide critical insights into how the system is likely to respond in the future, and hence has important implications for food security and resource management. Based on these findings, Chinese governments could better allocate resource and guide agricultural priorities to make full use of the favorable conditions and simultaneously avoid the terrible conditions. Future efforts should be focused towards assessments at finer spatial scales and cultivar specific temperature thresholds.

Acknowledges

This study was supported by the National Natural Science Foundation of China (Grant No. 41807506; 41201458), the Science and Technology Program of Hangzhou (Grant No. 20180432B12; 20150533B03) and Natural Science Foundation of Zhejiang (LQ18D010007; LY16D010007). National Key Research and Development Plan of China ((Grant No. 2016YFB0501404)

Appendix A. Supplementary data

Supplementary material related to this article can be found, in the online version, at doi:https://doi.org/10.1016/j.eja.2018.11.004.

References

Arshad, M.S., Farooq, M., Asch, F., Krishna, J.S., Prasad, P.V., Siddique, K.H., 2017. Thermal stress impacts reproductive development and grain yield in rice. Plant Physiol. Biochem. 115, 57–72.

Chen, C., Qian, C., Deng, A., Zhang, W., 2012. Progressive and active adaptations of cropping system to climate change in Northeast China. Eur. J. Agron. 38, 94–103.

Espe, M.B., Hill, J.E., Hijmans, R.J., McKenzie, K., Mutters, R., Espino, L.A., Linquist, B.A., 2017. Point stresses during reproductive stage rather than warming seasonal temperature determines yield in temperate rice. Glob. Change Biol. https://doi.org/10.1111/gcb.13719.

Field, C.B., Barros, V., Stocker, T.F., Dahe, Q., 2012. Managing the Risks of Extreme Events and Disasters to Advance Climate Change Adaptation: Special Report of the Intergovernmental Panel on Climate Change. Cambridge University Press.

Gourdji, S.M., Sibley, A.M., Lobell, D.B., 2013. Global crop exposure to critical high temperatures in the reproductive period: historical trends and future projections. Environ. Res. Lett. 8 (2), 024041.

Iizumi, T., Furuya, J., Shen, Z., Kim, W., Okada, M., Fujimori, S., Hasegawa, T., Nishimori, M., 2017. Responses of crop yield growth to global temperature and socioeconomic changes. Sci. Rep. 7, 7800.

Lesk, C., Rowhani, P., Ramankutty, N., 2016. Influence of extreme weather disasters on global crop production. Nature 529, 84–87.

Li, Z., Liu, Z., Anderson, W., Yang, P., Wu, W., Tang, H., You, L., 2015. Chinese rice production area adaptations to climate changes, 1949–2010. Environ. Sci. Technol. 49, 032–2037.

Liu, X., Zhang, Z., Shuai, J., Wang, P., Shi, W., Tao, F., Chen, Y., 2013. Impact of chilling injury and global warming on rice yield in Heilongjiang Province. J. Geogr. Sci. 23, 85–97.

Meng, Q., Hou, P., Lobell, D.B., Wang, H., Cui, Z., Zhang, F., Chen, X., 2014. The benefits of recent warming for maize production in high latitude China. Clim. Change 122 (1-2), 341–349.

Moura, D.S., Brito, G.G., Moraes, Í.L., Fagundes, P.R., Castro, A.P., Deuner, S., 2017. Cold tolerance in rice plants: phenotyping procedures for physiological breeding. J. Agric. Sci. 10, 313.

Olesen, J.E., Trnka, M., Kersebaum, K.C., Skjelvåg, A.O., Seguin, B., Peltonen-Sainio, P., Micale, F., 2011. Impacts and adaptation of European crop production systems to climate change. Eur. J. Agron. 34, 96–112.

Qian, W., Chen, Y., Jiang, M., Hu, Q., 2015. An anomaly-based method for identifying signals of spring and autumn low-temperature events in the Yangtze River valley, China. J. Appl. Meteorol. Climatol. 54 (6), 1216–1233.

Ren, G., Ding, Y., Tang, G., 2017. An overview of mainland China temperature change research. J. Meteorol. Res. 31 (1), 3–16.

Sánchez, B., Rasmussen, A., Porter, J.R., 2014. Temperatures and the growth and development of maize and rice: a review. Glob. Change Biol. 20, 408–417.

Stott, P., 2016. How climate change affects extreme weather events. Science 352, 1517–1518.

Sun, W., Huang, Y., 2011. Global warming over the period 1961-2008 did not increase high-temperature stress but did reduce low-temperature stress in irrigated rice across China. Agric. For. Meteorol. 151, 1193–1201.

Sun, Z., Wang, X., Yamamoto, H., Zhang, J., Tani, H., Zhong, G., Yin, S., 2017. Extraction of rice-planting area and identification of chilling damage by remote sensing technology: a case study of the emerging rice production region in high latitude. Paddy Water Environ. 15, 181–191.

Sun, Q., Yang, Z., Che, X., Han, W., Zhang, F., Xiao, F., 2018. Pricing weather index insurance based on artificial controlled experiment: a case study of cold temperature for early rice in Jiangxi, China. Nat. Hazards 91, 69–88.

Tao, F., Zhang, S., Zhang, Z., 2013. Changes in rice disasters across China in recent decades and the meteotological and agronomic causes. Region. Environ. Change 13, 743–759.

Wang, C.Y., 2008. Cold Damage of Crops in Northeast China. China Meteorological Press, Beijing, China, pp. 4.

Wang, P., Zhang, Z., Chen, Y., Wei, X., Feng, B., Tao, F., 2016. How much yield loss has been caused by extreme temperature stress to the irrigated rice production in China? Clim. Change 134, 635–650.

Yang, X., Lin, E., Ma, S., Ju, H., Guo, L., Xiong, W., Xu, Y., 2007. Adaptation of agriculture to warming in Northeast China. Clim. Change 84, 45–58.

Zhang, Z., Wang, P., Chen, Y., Song, X., Wei, X., Shi, P., 2014. Global warming over 1960–2009 did increase heat stress and reduce cold stress in the major rice-planting areas across China. Eur. J. Agron. 59, 49–56.

Zhang, L.W., Wang, X.Z., Jiang, L.X., Huang, J.F., 2015. Dynamic monitoring of rice delayed-type chilling damage using MODIS-based heat index in northeast China. J. Remote Sens. 19, 690–701 (in Chinese).

Zhang, Z., Chen, Y., Wang, C., Wang, P., Tao, F., 2017a. Future extreme temperature and its impact on rice yield in China. Int. J. Climatol. 37, 4814–4827.

Zhang, J., Zhang, Z., Tao, F., 2017b. Performance of temperature-related weather index for agricultural insurance of three main crops in China. Int. J. Disaster Risk Sci. 8, 78–90.

Zhao, C., Piao, S., Wang, X., Huang, Y., Ciais, P., Elliott, J., Liu, Y., 2017. Plausible rice yield losses under future climate warming. Nat. Plants 3, 16202.